JEE Journal of Ecological Engineering

Journal of Ecological Engineering, 2025, 26(8), 367–380
https://doi.org/10.12911/22998993/204005
ISSN 2299–8993, License CC-BY 4.0

Received: 2025.03.27
Accepted: 2025.05.26
Published: 2025.06.10

Synthesis of tannic acid and chitosan-modified magnetic graphene oxide nanocomposite for metal recovery in low-grade ore

Nadeem Raza[1], Muhammad Jamil[2], Zeeshan Ali[3*], Nicholas Wilkes[4], Muhammad Hayat[2], Tanveer Ul Haq[5], Muhammad Omar[6]

[1] Department of Chemistry, College of Science, Imam Mohammad Ibn Saud Islamic University (IMSIU), Riyadh, Saudi Arabia
[2] Institute of Chemical Sciences, Bahauddin Zakariya University, (BZU) Multan 60000, Pakistan
[3] Department of Climate Change MNS-University of Agriculture Multan MNSUAM, Pakistan
[4] Kamanjab 72 Limited REG # 14167772 Wenlock Road, London N1 7GU, England
[5] Department of Soil and Environmental Science MNS-University of Agriculture Multan MNSUAM, Pakistan
[6] Department of Electrical Engineering, Alain, UAE University, UAE
* Corresponding author's e-mail: zeeshan.ali@mnsuam.edu.pk

ABSTRACT

Mineral processing enhances ore value by removing gangue, making metal extraction cost-effective. A rapid and convenient method was developed for the extraction of Cu^{+2}, Mn^{+2} and Fe^{+2} using functionalized magnetic graphene oxide (MGO) obtained by coating graphene oxide (GO) with magnetic particles, modified with tannic acid (TA) and chitosan (Chi). The physical and chemical properties of magnetic nanocomposite (MGO- TA/Chi) were analyzed using various techniques, including UV/vis, FT-IR, SEM, XRD, and VSM. Atomic absorption and UV/vis spectroscopy were used to investigate the effective extraction of Mn^{+2}, Cu^{+2}, and Fe^{+2}. The adsorption performance data of MGO- TA/Chi under optimized conditions was evaluated through kinetic modeling. The maximum adsorption capabilities for Cu^{+2}, Mn^{+2}, and Fe^{+2} were observed at pH=5 from pregnant leached solution. With a magnetization value of 0.34 emu/g, MGO-TA/Chi showed a significant attraction to an external magnetic field which facilitated analyte separation. The synthesized magnetic nanocomposite showed 90.17, 87.23, and 85.24% adsorption for Cu^{+2}, Mn^{+2}, and Fe^{+2}, respectively. The adsorption process was spontaneous and endothermic, following the Langmuir adsorption model and pseudo-second-order kinetics. The findings demonstrate that TA/Chi-MGO is an effective adsorbent for the extraction of transition metal ions from leached solutions and could facilitate further in metallurgical processes.

Keywords: magnetic graphene oxide, nanocomposite, metals recovery, low-grade ore, adsorption.

INTRODUCTION

Most of metals, such as copper, manganese and iron – often referred to as backbone of industry – are extensively used in various technological applications due to their use in high-performance catalyst, electrical wiring, galvanization, alloys, stainless steel, and superconductors (Tong and Tong, 2011). Solar energy, known as photovoltaics, requires 11–40 times more copper per unit of electricity produced than traditionally deployed power generation methods, mainly from fossil fuels (Behar et al., 2021; Moreno-Leiva et al., 2020). Thus, switching towards solar energy will result in a substantial demand for copper. The final global copper demand is expected to rise from 24.3 Mt recorded in 2015 to 44.4 Mt in 2050 (Klose and Pauliuk, 2023). Likewise, manganese and its compounds are widely used in various industries including metallurgy, batteries, fertilizers, chemicals, pharmaceuticals, and particularly the steel industry. The demand for manganese constitutes over 90% of the total manganese consumption (Singh and Biswas, 2017). The addition of manganese is aimed to improve the strength, durability, and resistance of steel, with common quantities

ranging from 0.3 to 0.8% by weight (Kavitha and McDermid, 2012; Wang et al., 2023). According to the data from US Geological Survey (USGS), the total amount of manganese ore around the world in 2021 was 1.5 billion metric tons, mostly located in areas like Brazil, South Africa, and India (Cai et al., 2023; He et al., 2021; Wang et al., 2023). Iron is the most extensively used globally, as it is sturdy, cost-effective, and readily available from natural sources (Khatri et al., 2017). It can be molded into diverse shapes and retains its structural integrity even under applied force. Iron is crucial for human health, most of the iron in the human body is found in hemoglobin, a substance in red blood cells that transports oxygen all over the body (Gupta, 2014).

Extensive utilization of these metals for diverse aforementioned applications is exponentially exhausting the high grades ores and pressing much more stress on alternative sources. To this end, low grade ores are being explored for the beneficiation of metals; however, the greatest challenge associated with the cost-effective metal extraction from low grade ores is still in quest. Numerous strategies, including gravity separation, magnetic separation, chemical reactivity, flotation and leaching, are employed to extract metals from low grade ores [9]. In gravity separation, crushed ore is mixed with a liquid or gas, causing the heavier components to sink first, thus permitting valuable materials to become more concentrated, which can be easily gathered. Equipment like the Falcon gravity concentrator and the Condor dense medium separator employ gravity-based separation technique to efficiently recover valuable metals. However, gravity separation, relying on the differences in particle size and density between materials, is inappropriate for minerals with comparable densities or for minerals with extremely small particle sizes (Das and Sarkar, 2018; Izerdem and Ergun, 2024). In magnetic separation, magnetic minerals such as magnetite can be extracted from non-magnetic rocks by employing an electromagnetic separation device. However, the drawback of magnetic separation is that it does not work well with non-magnetic or less magnetic materials like graphite and gold (Hu et al., 2023; Rossi et al., 2014). Furthermore, secondary quantification techniques are required because magnetic separation is not a quantitative procedure (Ludwig et al., 2013). In chemical reactivity method of mineral recovery, certain chemicals can react differently with various minerals and metals in an ore (Rawlings, 2005). For example, cyanide leaching is a common technique for recovering gold from ore (Aylmore, 2016). However, this method demands bulk quantities of toxic chemicals and materials handling is also a significant problem (Kaya, 2016). In the flotation process, chemicals are employed to make the target minerals water-repellent, enabling them to cling to air bubbles and rise to the surface. However, this method is characterized by high consumption of reagents; thus, it is more costly than alternative separation techniques, and requires high maintenance costs which make flotation approach expensive and environment unfriendly (Falconi et al., 2023; Rao and Finch, 1989). In contrast to flotation, leaching process employs chemical solutions to dissolve and extract valuable metals which can subsequently be retrieved from the resulting solutions (Ding et al., 2024; Zhu et al., 2024). Leaching offers mining companies a sustainable, effective, and economical approach, with lower emissions compared to furnaces (Cheng et al., 2024; Raza and Zafar, 2013). The affordable cost of the heap leaching process makes it a financially appealing option. Other benefits of this method are that it is easy to perform, requires less energy and is potentially less harmful. Many reducing agents are used to extract the metals from leached solutions, such as coke – having high carbon content –used for the extraction of zinc and iron (Geet al., 2024; Raza et al., 2015). Many organic extractants like ACORGA and Lix are also being used to extract metals from leached solutions (Chepushtanova et al., 2024). In recent studies, several materials have been synthesized for extortion of metals. For instance, Ranjbar et al. extracted gold from copper anode residue by using a unique process involving magnetite nanoparticles (MNPs) (Ranjbar et al., 2014). Mattila and colleagues (2014) used a practical method to create magnetic cobalt nanoparticles coated with a thin carbon layer (Co@C NPs) for the extraction of gold ions (Mattila et al., 2014). Recently, agriculture and biomass based adsorbents (more economical and environment friendly) are being used in leached solution for metal recovery (Hosseinkhani et al., 2023). Recently, magnetic graphene oxide (MGO) was synthesized for the extraction of Cr, Cu, Zn and Ni (Farooq and Jalees, 2020). This material gave higher adsorption results but was reusable for four cycles only and rapidly lost its efficiency. From several other findings, it was

inferred that biomass-modified MGO is a promising material for the recovery of demanding metals nowadays in research due to high adsorption capacity, magnetic separation and sustainability. However, synthesis of modified MGO follows a complex procedure due to interference from co-existing ions and also its stability is also reduced over multiple cycles.

In this research, MGO-TA/Chi was used as an adsorbent to extract manganese, copper, and iron, and it showed high adsorption efficiency with the ability to be reused effectively. Tannic acid and chitosan are plant-derived non-toxic and highly functional materials having -COOH, -OH, -NH_2 and C=O groups. These functional materials have high selectivity for the recovery of important metals like copper, silver, iron, gold and chromium (Krzyzowska et al., 2017; Sharifiaghdam et al., 2022). Furthermore, MGO-TA/Chi has high carbon content as well as magnetic properties, which make it highly suitable for the extraction of metals from low grade ores. The objective of this research was to blend graphene with magnetic nanoparticles, and then modify their surface using tannic acid and chitosan, with the goal of improving their capability to extract metal ions from leached solution, making it a convenient and efficient method. MGO-TA/Chi adsorption potential was assessed using thermodynamic analysis, kinetics, and isotherms. The schematic illustration of synthesis and application of MGO-TA/Chi is given in Figure 1.

MATERIAL AND METHODS

Chemicals

Low-grade ore samples were taken from Khawazakhela, Swat, in Khyber Pakhtunkhwa, Pakistan, using normal sampling methods as described in authors' previous study (Ali et al., 2025). Briefly, the samples were carefully cleaned, followed by crushing using a jaw crusher and grinding using a ball mill to achieve an appropriate particle size. Afterwards, a steel mortar and pestle were used to convert the above ground material into a very fine powder as presented in Figure S1 (Appendix) (Ali et al., 2025). All the chemicals, including tannic acid ≥ 99%, chitosan (≥ 95%), ninhydrin powder, graphite powder 99.99%, potassium permanganate (lab grade ≥ 98%), sodium hydroxide pellets 98%, ferrous sulfate hexahydrate 99.5%, ferric chloride hexahydrate (99.99%), sulfuric acid (≥ 99.5%), hydrochloric acid (38%), hydrogen peroxide (30%), phosphoric acid, ammonia solution (34%), and methanol (99.9%), were purchased from Sigma Aldrich, Germany.

Synthesis of graphene oxide

The synthesis of graphene oxide (GO) was executed using Hummer's approach published elsewhere (Sajjad et al., 2024; Vanumamalai et al., 2025). Briefly, 3 mL of concentrated phosphoric acid and 27 mL of hydrochloric acid were mixed in a 250 mL beaker and stirred for

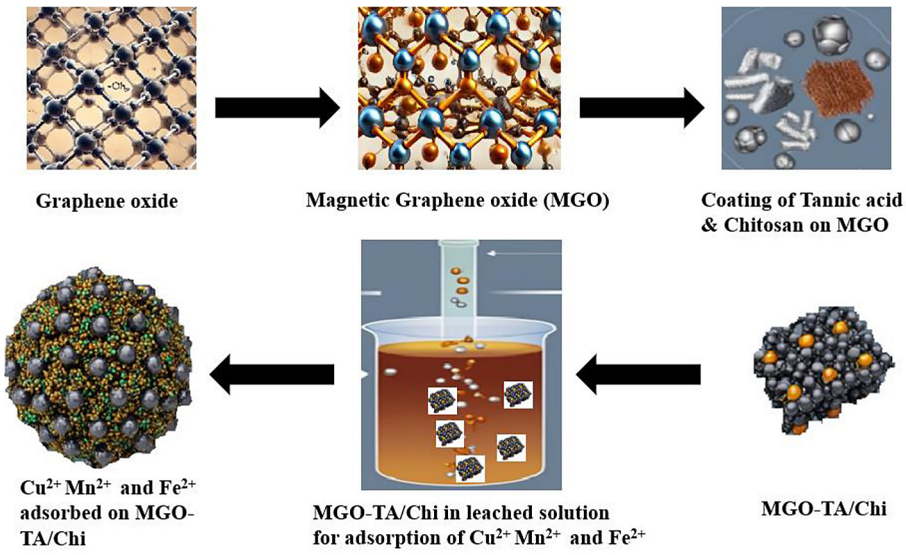

Figure 1. Schematic illustration for the synthesis of MGO-TA/Chi and adsorption of metals from leached solution of low-grade ore

30 minutes. Graphite powder (0.25 g) was then added quickly, followed by the gradual addition of 1.32 g potassium permanganate. The mixture was stirred for 6 hours, resulting in a color change from black to dark green. Hydrogen peroxide was added dropwise to the above-mentioned solution, stirred for 10 minutes and cooled. The supernatant was discarded, and the graphene oxide residue was washed repeatedly with 0.1 M hydrochloric acid and deionized water. Finally, the residue was dried for 24 hours at 90 °C.

Synthesis of iron oxide nanoparticles

The iron oxide nanoparticles were synthesized using the co-precipitation method (Ali et al., 2024). Briefly, 100 mL of 0.1 M $FeSO_4 \cdot 7H_2O$ and 100 mL of 0.2 M $FeCl_3 \cdot 6H_2O$ were mixed, gently stirred while heating at 80 °C for 40 minutes. Then, 20 mL of 0.1 M ammonia solution was slowly added to achieve pH 10 to precipitate iron oxide nanoparticles. The precipitates were filtered, washed with deionized water, and dried in an oven at 90 °C for 12 hours and stored in glass vials for subsequent analysis.

Synthesis of magnetic graphene oxide

A solution of ferric chloride hexahydrate (0.1 M) and a solution of ferrous sulfate heptahydrate (0.05 M), both 100 mL each, were added in a round bottom flask followed by the addition of the above-mentioned synthesized graphene oxide (1 g) and stirred at 90 °C for 40 minutes. After adding 20 mL of 0.1 M ammonia solution dropwise, magnetic graphene oxide precipitates were formed at pH 10, filtered, washed with deionized water, and dried in an oven at 90 °C for 12 hours (Sajjad et al., 2024).

Preparation of Fe_3O_4-GO-tannic acid-chitosan composite film

Firstly, chitosan solution was prepared by dissolving 0.1 g of chitosan in 10 mL of 0.1 M acetic acid solution and heating at 90 °C with continuous stirring until the solids completely dissolved. Secondly, 0.1 g of tannic acid was dissolved in 10 mL deionized water and heated at 90 °C with constant stirring, until it was fully dissolved. The tannic acid solution was then gradually added to the chitosan solution, and the mixture was stirred while heating at 90 °C for 30 minutes. Subsequently, 40 mg of magnetic graphene oxide was introduced into the above-mentioned solution and mixed for another 30 minutes under the same conditions. The resulting Fe_3O_4-GO-tannic acid-chitosan solution was spread as a thin layer in a petri dish and allowed to cool at room temperature. Finally, the Fe_3O_4-GO -TA/Chi composite was dried for 48 hours in an oven at 60 °C, and the resulting thin film was peeled off and cut into pieces using a puncher.

Leaching and adsorption process

The leaching experiments were carried out in a 100 ml glass beaker. A magnetic stirrer was used to mix the solutions, ensuring consistent mixing and mass transfer during the kinetic tests. A standard experiment involved adding 2 g low grade ore powder into the beaker along with the selected acid volume (0.25 M H_2SO_4 and 30% H_2O_2). The magnetic stirrer was set to a constant speed of 300 rpm for all tests. After the leaching process, pregnant leach solution (PLS) was filtered using a membrane filter paper (pore size 0.45 µm, diam. 47 mm) under ambient conditions. The PLS volume was then diluted to 100 ml by adding deionized water and stored in a beaker for adsorption of Cu^{+2}, Mn^{+2} and Fe^{+2} by the above-mentioned synthesized adsorbent (MGO-TA/Chi). The pH of the leached solution was maintained using 0.25 M NaOH. After that, 1 g of MGO-TA/Chi was added to 100 mL leached solution and placed on shaker for 1hour. Afterwards, MGO-TA/Chi loaded with metals was separated by applying external magnetic field and adsorbed metal ions were eluted using 0.1 M HNO_3 and were analyzed using atomic absorption spectrophotometer.

Characterization

Various analytical techniques were employed to characterize the MGO-TA/Chi composite. The spectrophotometric studies were performed using Shimadzu UV1800 ENG 240 V, SOFT P/N 206–25400-58. The functionalities present in MGO-TA/Chi were determined by using FTIR (CHNO/S 2400 from PerkinElmer, USA). An atomic absorption spectrophotometer (AAS, Aurora Biomed ICR8000) was employed to quantify Cu^{+2}, Mn^{+2} and Fe^{+2} in leached solution using a hollow cathode lamp as an excitation source and fuel-air ratio of 2:10 L min^{-1}. Morphological and elemental details of the MGO-TA/Chi

and low-grade ore were obtained using a scanning electron microscope equipped with energy-dispersive X-ray spectroscopy (SEM-EDX, SEM; JOEL; Japan) and Evo LS 10 Zeiss Germany. The phase angle of the synthesized material was characterized by an X-ray diffractometer (XRD, Bruker D8) for more precise identification and quantification of material phases. XRD was scanned at 2θ from 4 to 80°, with Cu kα radiation.

RESULTS AND DISCUSSION

FTIR analysis

The FTIR analysis revealed the functional groups present in the adsorbent materials. The FTIR spectrum of graphene oxide (GO) showed a broad peak in the 3600–3300 cm^{-1} region, indicating the presence of hydroxyl and carboxylic groups. Other peaks at 1620, 1390, and 1025 cm^{-1} were attributed to C=O, C-H, and C-O, respectively, as given in Figure 2a. The FTIR spectrum of magnetized graphene oxide (MGO) exhibited a prominent peak at 3550 cm^{-1}, suggesting the presence of hydroxyl groups from carboxylic functional groups, and a peak around 1690 cm^{-1} indicating the C=O of carboxylic groups. Additional peaks at 1568, 1434, 1020, and 580 cm^{-1} were assigned to C=C, C-H, C-O, and Fe-O, respectively, see Figure 2b. The strong peak at 580 cm^{-1} confirmed the presence of Fe-O coating on the GO. The FTIR spectrum of the MGO-TA/Chi composite in Figure 2c showed similar peaks to its individual components, with additional absorption bands at around 2921 and 2877 cm^{-1} attributed to the C-H symmetric and asymmetric stretching of chitosan.

Microscopic and EDX analysis

The scanning electron microscope (SEM) was employed to study the surface characteristics of MGO and TA/Chi-MGO and low-grade ore particles. The SEM images (Figure 3a and b) of the MGO and MGO-TA/Chi samples showed agglomerated structure that resembled elongated or irregularly shaped particles, which is common in graphene-based nanomaterials. Furthermore, particles with irregular shapes and diverse sizes were also observed. The SEM image (Figure S2a) display the uneven distribution of irregularly shaped low-grade ore particles with bar scale of 1 µm (Ali et al., 2025). Furthermore, bar scale of 1 µm in SEM image indicates agglomeration of graphene based magnetic nanoparticles.

EDX, being a widely used analytical technique for elemental analysis, was selected to determine the chemical composition of the MGO and MGO-TA/Chi (Figure 3c and d). The spectrum confirmed the presence of carbon as a major element (63%) incorporated by graphene oxide and iron particles. Oxygen, nitrogen, and silicon were detected with the percentage values of 29, 3, and 5%, respectively. The EDX spectrum of the low-grade copper ore sample shows the

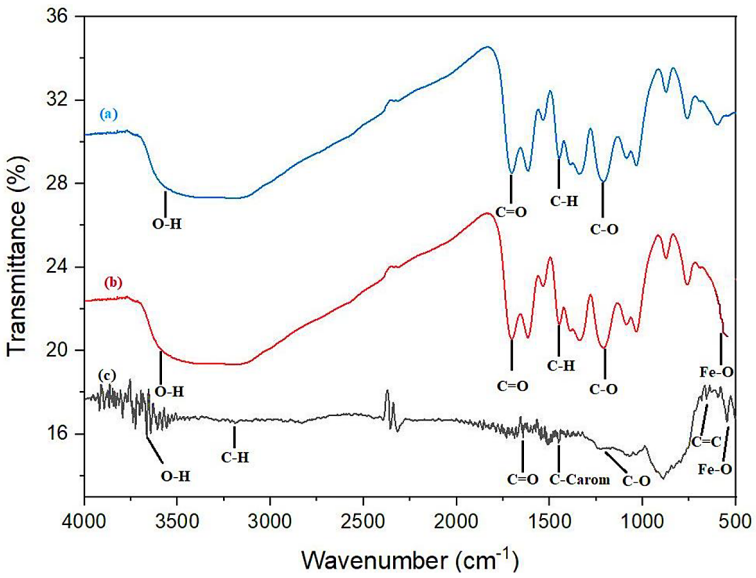

Figure 2. FT-IR analysis of GO (a), MGO (b) and MGO- TA/Chi (c)

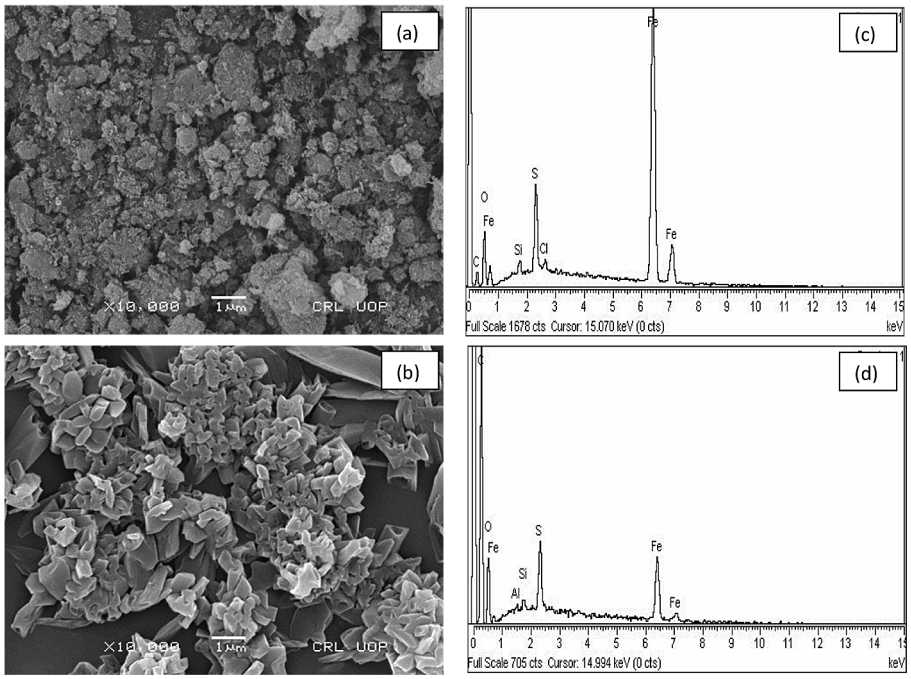

Figure 3. SEM images and EDX spectrum of MGO (a, c) and MGO-TA/Chi (b, d)

elemental composition, as illustrated in Figure S2b (Appendix). Additionally, Table S1 (Appendix) displays the semi-quantitative data of the chemical components present in the low-grade ore sample (Ali et al., 2025).

X-ray diffraction studies

The crystalline structure of MGO and MGO-TA/Chi materials was determined using X-ray diffraction analysis, as displayed in Figure 4a and 4b. The diffraction patterns observed in the range of 10° to 80° (at angles such as 10°, 30°, 35°, 43.5°, 53.6°, and 63°) corresponded to the crystalline planes (0 0 2), (101), (2 2 0), (3 1 1), (4 0 0), (4 2 2), and (4 4 0), respectively, which matches the typical XRD data for the spinel structure of Fe_3O_4 (JCPDS 19–0629) and magnetic graphene oxide nanoparticle spectrum (Sajjad et al., 2024). Meanwhile, the XRD pattern of MGO-TA/Chi (Figure 4b) is similar to MGO (Figure 4a) spectrum with low signal intensity. The strength of the signals or peaks declines when moving from MGO to MGO-TA/Chi, suggesting that tannic acid and chitosan have covered the MGO surface. The amorphous nature of the composite suggests the increased adsorption capability of the adsorbent. The XRD pattern of low-grade ore confirmed the presence of chalcopyrite (CODB No. 2104753) as the dominant Cu and Fe-bearing mineral phases and it was already presented in authors' previous study (Ali et al., 2025). The peaks around 30°, 35°, 50°, 53.6° and 58°corresponded to Cu and Fe species in chalcopyrite. The signals of Mn were obscured by Fe due to its low concentration.

Magnetic study

The magnetic characteristics of GO, MGO, and MGO- TA/Chi composite was examined using vibrating sample magnetometer VSM, and the findings are displayed in Figure 5 (a–c). Due to their nonmagnetic composition, GO without any coatings or alterations revealed the zero-magnetization value (Figure 5a). Notably, the overall magnetization value of GO is increased from zero to 0.6 emu/g due to its binding with iron oxide which is magnetic material (Figure 5b). After the addition of Chi and TA, it was found that the magnetization of MGO had significantly decreased 0.23 emu/g (Figure 5c). Magnetic characteristics of MGO were greatly diminished after the addition of various non-magnetic layers such as tannic acid and chitosan but the MGO- TA/Chi composite was still sufficiently magnetic and responsive to external magnetic field and this response significantly helped in separation of metals from the aqueous solution containing metals.

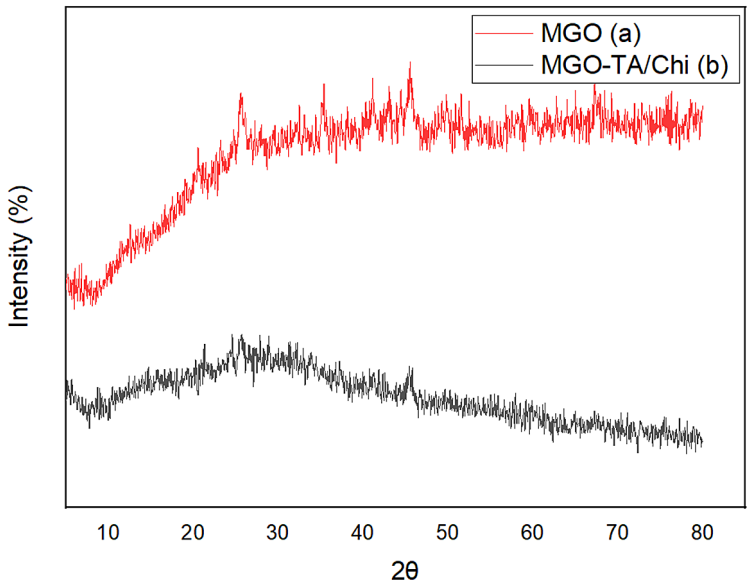

Figure 4. XRD pattern of MGO (a), MGO-TA/Chi (b)

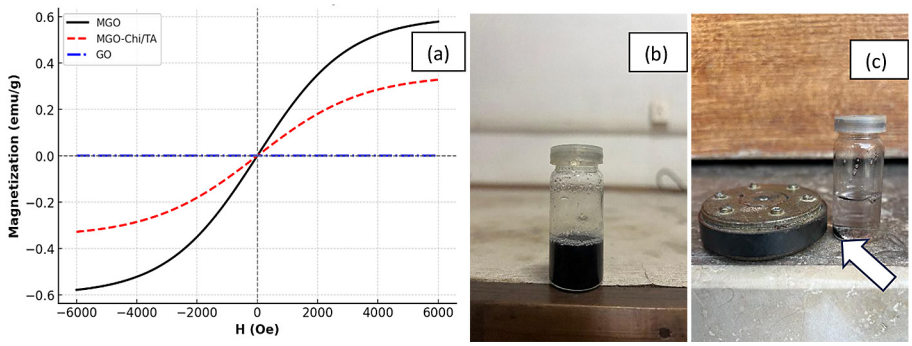

Figure 5. Magnetization values of GO, MGO, MGO-TA/Chi (a) and images (b and c) of nanocomposite showing attraction towards magnet

Adsorption isotherm of MGO-TA/Chi

Understanding adsorption isotherms is essential for knowing how adsorption process of targets on a specific adsorbent works. These isotherms give key information about how adsorbate molecules are distributed between the solid and liquid phases. Different isotherms can be used to describe the adsorption of heavy metals on various adsorbents. Figure 6 shows the Langmuir and Freundlich isotherm plots for the adsorption of heavy metals using the tannic acid and chitosan-modified magnetic graphene oxide nanocomposite (MGO-TA/Chi). Table 1 summarizes the Langmuir and Freundlich constants for adsorption of heavy metals through MGO-TA/Chi.

The Langmuir adsorption capacities of MGO-TA/Chi for copper (Cu^{2+}), manganese (Mn^{2+}), and iron (Fe^{2+}) were 90.17 mg g^{-1}, 87.23 mg g^{-1} and 85.24 mg g^{-1}, respectively. This shows that the adsorption of these metal ions onto MGO-TA/Chi occurs in a single layer on the surface. The "R_L" separation factor calculated using the Langmuir constant and initial metal ion concentration helps understand the strength of the interaction between the adsorbate and adsorbent. When R_L is less than 1, it means the adsorption is favorable (Ali et al., 2023). For copper, manganese, and iron, the R_L values were between 0 and 1, showing that the adsorption of these metals on MGO-TA/Chi is favorable.

The Freundlich adsorption capacities for copper, manganese, and iron were 117.10 mg g^{-1}, 73.30 mg g^{-1}, and 70.20 mg g^{-1}, respectively. The Freundlich model supports the idea that adsorption happens on an adsorbent surface with different types of sites.

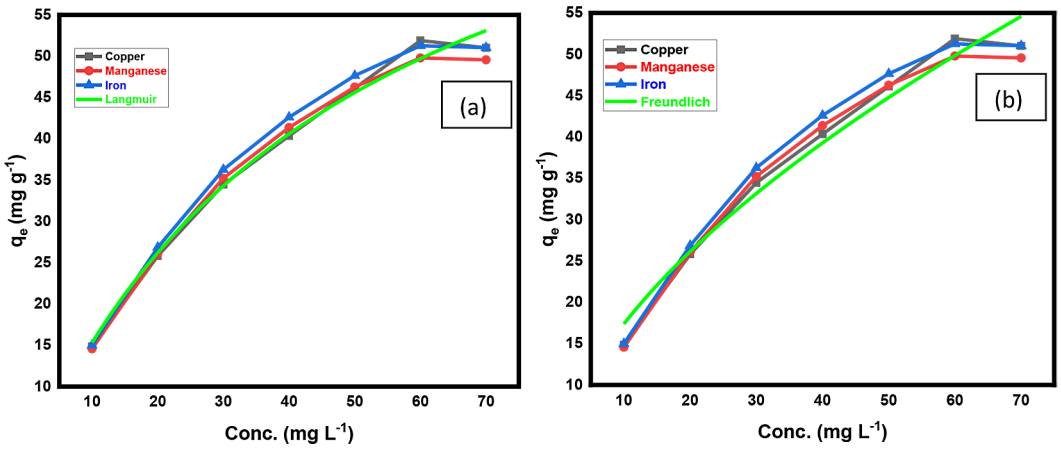

Figure 6. Langmuir isotherm (a) Freundlich isotherm (b) for extraction of Cu^{2+}, Mn^{2+}, and Fe^{2+} by MGO-TA/Chi

Table 1. Adsorption kinetic parameters obtained using non-linear Langmuir and Freundlich models for, Cu^{+2}, Mn^{+2} and Fe^{+2}metal ions on MGO-TA/Chi

Sr. No.	Langmuir			Freundlich			
Non-Linear modeling	q_{exp}(mg/g)	q_m(mg/g)	K_L(L mol^{-1})	R^2	q_m(mg/g)	N	R^2
Copper	90	90.17	0.020	0.992	117.10	1.70	0.975
Manganese	88	87.23	0.027	0.990	73.30	1.68	0.956
Iron	86	85.24	0.023	0.991	70.20	1.79	0.961

In conclusion, MGO-TA/Chi efficiently adsorbs Cu, Mn and Fe ions, and both Langmuir and Freundlich models show that it works well for removing these heavy metals from water.

Kinetic study

Kinetic-based models, such as pseudo-first-order (PFO) and pseudo-second-order (PSO), were applied to explore the adsorption mechanisms and the steps limiting adsorption rates. Various kinetic models, both linear and non-linear with differing degrees of complexity are commonly used. Non-linear modeling is considered superior to linear modeling, because it provides more realistic kinetic parameters (Ali et al., 2023). Additionally, it allows for the assessment of all models, offering a more accurate comparison to determine which model best reflects a specific kinetic dataset. By using non-linear modeling, the discontinuity of models and the determination of parameters before optimum time for adsorption can be minimized.

The low value of χ^2, the high value of R^2, and the correlation of experimental q_e values to the calculated q_e values indicate the best fitting of a kinetic model for adsorption studies (Hayat et al., 2022; Hayat et al., 2025). A non-linear approach using both PFO and PSO models was applied to analyze the kinetic data (Figure 7).

For copper, the non-linear PSO model showed a high R^2 value of 0.995 and a low χ^2 value of 0.108, with the calculated q_e value close to the experimental value of 89.31 mg g^{-1}. Manganese followed a similar trend, with an R^2 value of 0.993 and χ^2 of 0.153, yielding a q_e of 87.71 mg g^{-1}. The PSO model also provided excellent fitting for iron with an R^2 of 0.996, a χ^2 of 1.39, and a q_e value of 85.44 mg g^{-1} as given in Table 2. These results further confirm that Cu, Mn and Fe ion's adsorption on MGO-TA/Chi follows a pseudo-second-order kinetic model, indicating a chemosorption process with strong ionic interactions between the metal ions and the adsorbent.

Effect of pH on adsorption of metal ions

The pH of the aqueous medium influences both the ionic state of the functional groups on the adsorbent surface and the metal ions present in the leached solution. The adsorption of Cu^{+2}, Mn^{+2} and Fe^{+2} on the surface of MGO-TA/Chi was investigated at different pH levels ranging from 2.0 to 8.0, as given in Figure 8. The

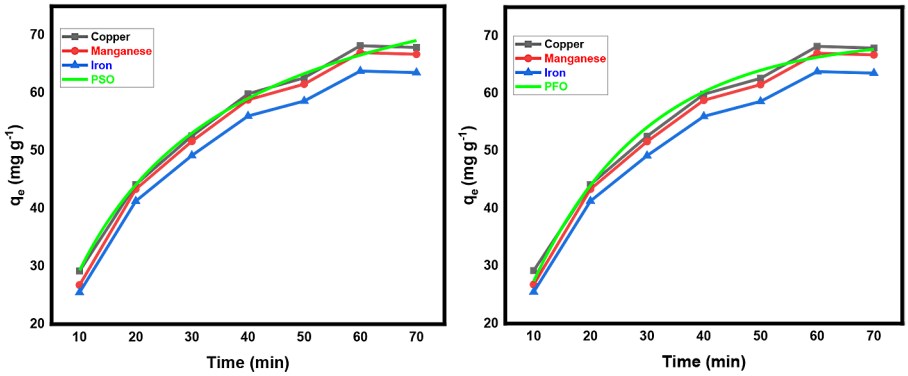

Figure 7. Kinetic modeling for extraction of Cu^{2+}, Mn^{2+}, and Fe^{2+} by using MGO-TA/Chi

Table 2. Adsorption kinetic parameters obtained using the pseudo-first order and pseudo-second-order models for Cu^{+2}, Mn^{+2} and Fe^{+2} metal ions on MGO-TA/Chi

Sr. No.	Pseudo-1st order			Pseudo-2nd order		
Non-Linear modeling	R^2	χ2	q_e (mg/g)	R^2	χ2	q_e(mg/g)
Copper	0.985	2.30	69.50	0.995	0.108	89.31
Manganese	0.987	1.98	64.70	0.993	0.153	87.71
Iron	0.979	2.2	65.96	0.996	1.39	85.44

adsorption investigation was carried out using 1 g of adsorbent, a contact time of 35 minutes, and an initial metal concentration of 150 mg/L.

The observed increasing trend in adsorption rates of Cu^{2+}, Mn^{2+}, and Fe^{2+} ions with increasing pH levels can be attributed to changes in both the adsorbent surface charge and the availability of functional groups for electrostatic interactions. At low pH levels (pH < 2.0), the high concentration of hydrogen ions (H^+) leads to protonation of the adsorbent surface and its functional groups, resulting in a positively charged adsorbent surface. This positive charge creates electrostatic repulsion between the adsorbent and the metal

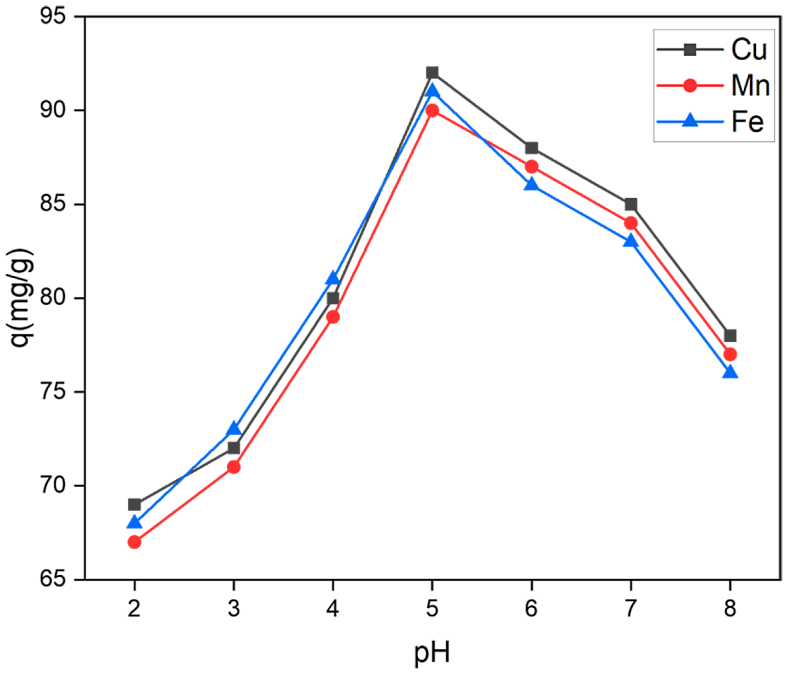

Figure 8. Effect of pH on the uptake of Cu^{2+}, Mn^{2+}, and Fe^{2+} using MGO-TA/Chi

cations (Cu^{2+}, Mn^{2+}, Fe^{2+}), thereby hindering effective adsorption. However, as the solution pH increases, the concentration of H^+ decreases, leading to deprotonation of the adsorbent's functional groups, a net negative charge is created on the adsorbent surface, enhancing electrostatic attraction between the negatively charged adsorbent surface and the positively charged metal cations (Zenasni et al., 2012). Similarly, higher pH values make heavy metal ions generate insoluble hydroxide precipitates (such as $Cu(OH)_2$, $Fe(OH)_2$, and $Mn(OH)_2$), which are found in many metals such as Cu^{2+}, Mn^{2+}, and Fe^{2+}. As a result, there are less free metal ions in solution accessible for adsorption onto the MGO-TA/Chi surface, which lowers process efficiency. Consequently, the adsorption capacity for these target metal ions is significantly increased, from 20 to 25%, as the pH range shifts from 4.0 to 5.0 and decreased 13 to 15% when moving from 5 to 8.

AAS analysis

After leaching, the concentrations of Cu^{2+}, Mn^{2+}, and Fe^{2+} in the PLS were determined using AAS, yielding values of 13.01 mg/L, 17.1 mg/L, and 623.24 mg/L, respectively. Notably, due to the high concentration of iron, the Fe^{2+} solution required a 1:100 dilution prior to measurement so after dilution Fe concentration was 6.23mg/L. Subsequently, the MGO-TA/Chi nanocomposite was employed to extract these metal ions from the PLS. When 0.5 g of the nanocomposite was mixed with 50 mL of the sample and agitated for 2 hours, it achieved adsorption efficiencies of 90.17% for Cu^{2+}, 87.23% for Mn^{2+}, and 85.24% for Fe^{2+} ions given in Figure 9.

These findings underscore the efficacy of the nanocomposite in adsorbing appreciable amounts of metal ions from the PLS. However, the observed extraction rates are slightly lower compared to those obtained with synthetic solutions

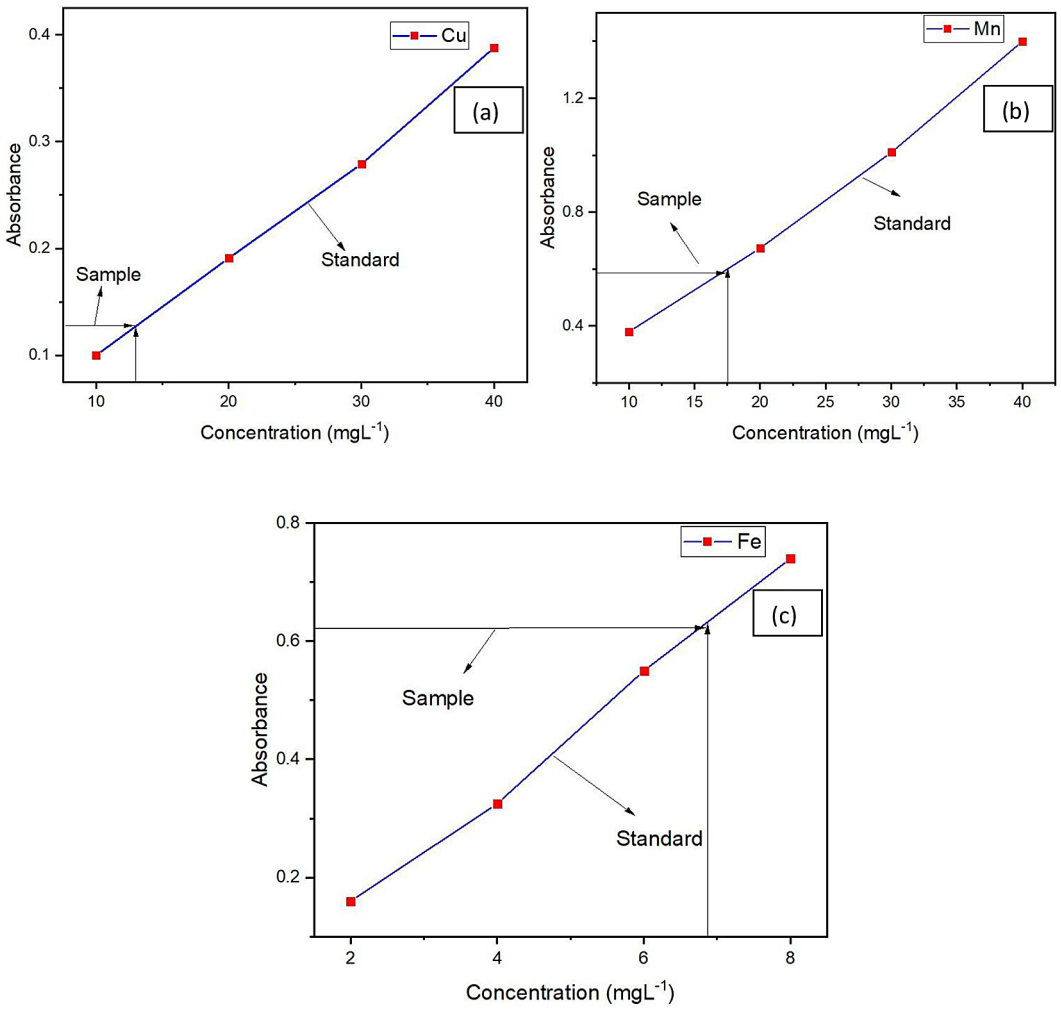

Figure 9. Calibration curves for Cu (a), Mn, (b) and Fe (c) using AAS

(Zou et al., 2024). This discrepancy is likely attributed to the presence of competing ions in the natural ore sample, which can interfere with the adsorption process. These observations align with the current findings, suggesting that while the MGO-TA/Chi nanocomposite is effective, its performance can be impacted by the complex composition of natural leach solutions.

Regeneration study

To enhance the efficiency and cost-effectiveness of the adsorption process, researchers focus on regenerating adsorbents through desorption techniques. This procedure allows for the recovery of the adsorbate, reduces the need for new adsorbents, stabilizes the adsorbents, and provides insights into the reversibility of the adsorption process. In the case of regenerating modified magnetic graphene oxide nanocomposites, dilute solutions of nitric acid (HNO_3) or hydrochloric acid (HCl) are commonly used (Wani et al., 2024). The hydronium ions from these acids compete with the adsorbed metal ions for the active sites, effectively displacing the metal ions and clearing the active sites for reuse in future adsorption cycles. For the current study, 0.1 M HNO_3 was used to facilitate the desorption of adsorbed metal ions, explicitly targeting Cu^{2+}, Mn^{2+}, and Fe^{2+} from modified magnetic graphene oxide nanocomposites.

In the regeneration process, 0.7 g of the dried modified MGO-TA/Chi nanocomposite was added to 50 mL of a metal ion solution (140 mg/L of Cu^{2+}, Mn^{2+}, and Fe^{2+}). The mixture was stirred at 100 rpm for 1 hour to reach adsorption equilibrium. Afterwards, the metal-loaded nanocomposite was submerged in 0.1 M HNO_3 for 2 hours while being stirred to ensure the thorough desorption of the metal ions from the nanocomposite surface. The desorption efficiency for Cu, Mn and Fe was evaluated over five cycles to determine the stability and reusability of the modified magnetic graphene oxide nanocomposite and given in Table 3.

Comparative study

To increase the adsorption of metals, several adsorbents have been synthesized. Out of these synthesized adsorbents magnetic graphene oxides (MGO) based adsorbents gave remarkable good results as compared to traditionally designed materials. In this study, a novel tannic acid and chitosan coated MGO material was synthesized

Table 3. Regeneration study of MGO-TA/Chi by calculating desorption efficiency

Desorption efficiency (%) of MGO-TA/Chi			
No.	Cu^{2+}	Mn^{+2}	Fe^{+2}
1	93.89	91.17	93.61
2	89.81	88.75	91.65
3	87.11	86.50	88.60
4	85.20	84.67	86.34
5	83.56	83.70	85.98

Table 4. Adsorption comparison of MGO-TA/Chi as compare to previously synthesized MGO materials

Serial No.	Modified MGO nanomaterial	Type of water sample	Adsorption efficiency (%)	Ref
1	(MGO) synthesized via co-precipitation	Synthetic water sample	Ni^{2+}: 85%, Zn^{2+}: 88%, Cu^{2+}: 87%	(Farooq and Jalees, 2020)
2	(MGO)	Synthetic water sample	Cu^{2+}: 80%, Pb^{2+}: 85%, Cd^{2+}: 75%	(Hur et al., 2015)
3	$NiFe_3O_4$/Graphene Oxide Nanocomposite	Synthetic water sample	Cr^{3+}: 89%	(Gao et al., 2011)
4	Graphene Oxide with dual magnetic behavior	Synthetic water sample	Cu^{2+}: 85%, Pb^{2+}: 88%	(Melchor-Durán et al., 2024)
5	Organo-functionalized MGO	Environmental water sample	Ni^{2+}: 82%, Cd^{2+}: 78%	(Sherlala et al., 2018)
6	MGO with amino functionalization	Pharmaceutical effluent	Pb^{2+}: 89%, Ni^{2+}: 87%, Cr^{6+}: 85%	(Gopalakrishnan, et al., 2015)
7	This work	Pregnant Leached Solution	Cu^{2+}: 90.17% Mn^{2+}: 87.23% Fe^{2+}: 85.24%	

and used as adsorbent in PLS. This MGO-TA/Chi gave excellent adsorption as compare of previous synthesized MGO based materials. The comparative study is given in Table 4.

CONCLUSIONS

In this study, a novel modified magnetic graphene oxide composite (MGO-TA/Chi) was successfully developed and utilized for the efficient extraction of copper, manganese, and iron from a pregnant leached solution of low-grade ore. The structural and chemical properties of the material were thoroughly characterized using FT-IR, SEM, EDX, and VSM, while metal removal efficiency was quantified through AAS and UV-vis spectrophotometry. MGO-TA/Chi demonstrated remarkable adsorption capacities, achieving 90.17% removal of Cu^{2+} (13.01 mg g^{-1}), 87.23% removal of Mn^{2+} (17.01 mg g^{-1}), and 85.24% removal of Fe^{2+} (6.23 mg g^{-1} after 100 times dilution). The adsorption process followed the Langmuir isotherm model, while the kinetics aligned with a pseudo-second order rate equation, indicating a chemisorption-dominated mechanism. Moreover, the adsorbent exhibited excellent reusability for five consecutive cycles, as metal ions could be fully recovered using a 0.1 M HNO_3 solution. These findings confirm that MGO-TA/Chi is an effective, reusable, and eco-friendly adsorbent for metal extraction from low-grade ore solutions, making it a promising candidate for sustainable wastewater treatment and resource recovery.

Acknowledgement

This research project was funded by Kamanjab 72 Ltd, UK. The authors are grateful to Nicholas Wilkes (Director Kamanjab) for funding this project. Special thanks to Dr. Saad Saleem Khan for his support in the project. All authors are thankful to Bahauddin Zakariya University for providing the lab facility to conduct this research.

REFERENCES

1. Ali, Z., Sajid, M., Ahmed, M. M., Hanif, M., Manzoor, S. (2024). Synthesis of green fluorescent cross-linked molecularly imprinted polymer bound with anti-cancerous drug (docetaxel) for targeted drug delivery. *Polymer Bulletin, 81*(1), 679–696.
2. Ali, Z., Sajid, M., Raza, N., Sohail, Y., Hayat, M., Manzoor, S., ... Ansari, M. Z. (2023). Study of modified biomass of Gossypium hirsutum as heavy metal biosorbent. *Arabian Journal of Chemistry, 16*(12), 105332.
3. Ali, Z., Wilkes, N., Raza, N., Omar, M. (2025). Modified Hydrometallurgical approach for the beneficiation of copper from its low-grade ore. *ACS Omega*. doi:10.1021/acsomega.4c09656
4. Aylmore, M. (2016). Alternative lixiviants to cyanide for leaching gold ores. In *Gold ore processing* 447–484. Elsevier.
5. Behar, O., Peña, R., Kouro, S., Kracht, W., Fuentealba, E., Moran, L., Sbarbaro, D. (2021). The use of solar energy in the copper mining processes: A comprehensive review. *Cleaner Engineering and Technology, 4*, 100259.
6. Cai, Y., Long, G., Xiao, Q., Ma, K., Zeng, X., Tang, Z., Wang, J. (2023). Effect of low temperature calcined electrolytic manganese residue on the early-age hydration of cement paste. *Construction and Building Materials, 387*, 131608.
7. Cheng, F., Zhang, Y., Zhang, G., Zhang, K., Wu, J., Zhang, D. (2024). Eliminating environmental impact of coal mining wastes and coal processing by-products by high temperature oxy-fuel CFB combustion for clean power Generation: a review. *Fuel, 373*, 132341.
8. Chepushtanova, T., Yessirkegenov, M., Mamyrbayeva, K., Akcil, A., Gaipov, T. (2024). Extraction of Copper from Pregnant Leach Solution (PLS) and Reduction of Crud Formation. *Mineral processing and extractive metallurgy review*, 1–13.
9. Das, A., Sarkar, B. (2018). Advanced gravity concentration of fine particles: A review. *Mineral processing and extractive metallurgy review, 39*(6), 359–394.
10. Ding, H., Yuan, S., Lei, S., Wang, W., Wen, G., Dong, Z. (2024). Technology and principle on preferentially selective lithium extraction for spent ternary lithium batteries: A review. *Separation and Purification Technology*, 129691.
11. Falconi, I. B. A., Junior, A. B. B., Baltazar, M. d. P. G., Espinosa, D. C. R., Tenório, J. A. S. (2023). An overview of treatment techniques to remove ore flotation reagents from mining wastewater. *Journal of Environmental Chemical Engineering, 11*(6), 111270.
12. Farooq, M. U., Jalees, M. I. (2020). Application of magnetic graphene oxide for water purification: heavy metals removal and disinfection. *Journal of Water Process Engineering, 33*, 101044.
13. Gao, W., Majumder, M., Alemany, L. B., Narayanan, T. N., Ibarra, M. A., Pradhan, B. K., Ajayan, P. M. (2011). Engineered graphite oxide materials for application in water purification. *ACS applied materials & interfaces, 3*(6), 1821-1826.
14. Ge, H., Xie, F., Wu, S., Wang, W. (2024). Biomass as a

clean reductant for recovery of zinc from zinc leaching residue. *Journal of Cleaner Production, 434*, 139926.

15. Gopalakrishnan, A., Krishnan, R., Thangavel, S., Venugopal, G., Kim, S.-J. (2015). Removal of heavy metal ions from pharma-effluents using graphene-oxide nanosorbents and study of their adsorption kinetics. *Journal of Industrial and Engineering Chemistry, 30*, 14–19.
16. Gupta, C. (2014). Role of iron (Fe) in body. *IOSR Journal of Applied Chemistry, 7*(11), 38–46.
17. Hayat, M., Manzoor, S., Raza, N., Abbas, A., Khan, M. I., Elboughdiri, N., ... Al Arni, S. (2022). Molecularly imprinted polymeric sorbent for targeted dispersive solid-phase microextraction of fipronil from milk samples. *ACS omega, 7*(45), 41437–41448.
18. Hayat, M., Manzoor, S., Raza, N., Raza, H., Javid, A., Ali, Z., ... Alomar, T. S. (2025). Amine-functionalized organically modified silica for the effective adsorption of Chlorpyrifos and Triazophos Residues from Orange juice. *Food Chemistry, 465*, 141967.
19. He, S., Jiang, D., Hong, M., Liu, Z. (2021). Hazard-free treatment and resource utilisation of electrolytic manganese residue: A review. *Journal of Cleaner Production, 306*, 127224.
20. Hosseinkhani, O., Hamzehlouy, A., Dan, S., Sanchouli, N., Tavakkoli, M., Hashemipour, H. (2023). Graphene oxide/ZnO nanocomposites for efficient removal of heavy metal and organic contaminants from water. *Arabian Journal of Chemistry, 16*(10), 105176.
21. Hu, Z., Lu, D., Zheng, X., Wang, Y., Xue, Z., Xu, S. (2023). Development of a high-gradient magnetic separator for enhancing selective separation: A review. *Powder Technology, 421*, 118435.
22. Hur, J., Shin, J., Yoo, J., Seo, Y.-S. (2015). Competitive adsorption of metals onto magnetic graphene oxide: comparison with other carbonaceous adsorbents. *The Scientific World Journal, 2015*(1), 836287.
23. Izerdem, D., Ergun, S. L. (2024). Investigation of the effects of particle size on the performance of classical gravity concentration equipment. *Mineral processing and extractive metallurgy review, 45*(3), 155-172.
24. Kavitha, R., McDermid, J. R. (2012). On the in-situ aluminothermic reduction of manganese oxides in continuous galvanizing baths. *Surface and Coatings Technology, 212*, 152–158.
25. Kaya, M. (2016). Recovery of metals and nonmetals from electronic waste by physical and chemical recycling processes. *Waste Management, 57*, 64–90.
26. Khatri, N., Tyagi, S., Rawtani, D. (2017). Recent strategies for the removal of iron from water: A review. *Journal of Water Process Engineering, 19*, 291–304.
27. Klose, S., & Pauliuk, S. (2023). Sector-level estimates for global future copper demand and the potential for resource efficiency. *Resources, Conservation and Recycling, 193*, 106941.
28. Krzyzowska, M., Tomaszewska, E., Ranoszek-Soliwoda, K., Bien, K., Orlowski, P., Celichowski, G., Grobelny, J. (2017). Tannic acid modification of metal nanoparticles: Possibility for new antiviral applications. In *Nanostructures for oral medicine.* 335–363. Elsevier.
29. Ludwig, P., Egli, R., Bishop, S., Chernenko, V., Frederichs, T., Rugel, G., ... Orgeira, M. J. (2013). Characterization of primary and secondary magnetite in marine sediment by combining chemical and magnetic unmixing techniques. *Global and Planetary Change, 110*, 321–339.
30. Mattila, P., Heinonen, H., Loimula, K., Forsman, J., Johansson, L.-S., Tapper, U., ... Jokiniemi, J. (2014). Scalable synthesis and functionalization of cobalt nanoparticles for versatile magnetic separation and metal adsorption. *Journal of nanoparticle research, 16*, 1–11.
31. Melchor-Durán, A., Moreno-Virgen, M., Bonilla-Petriciolet, A., Reynel-Ávila, H., Lucio Ortiz, E., González-Vázquez, O. (2024). Heavy metal removal from water using graphene oxide in magnetic-assisted adsorption systems: characterization, adsorption properties, and modelling. *Separations, 11*(10), 294.
32. Moreno-Leiva, S., Haas, J., Junne, T., Valencia, F., Godin, H., Kracht, W., ... Eltrop, L. (2020). Renewable energy in copper production: A review on systems design and methodological approaches. *Journal of Cleaner Production, 246*, 118978.
33. Ranjbar, R., Naderi, M., Omidvar, H., Amoabediny, G. (2014). Gold recovery from copper anode slime by means of magnetite nanoparticles (MNPs). *Hydrometallurgy, 143*, 54–59.
34. Rao, S., Finch, J. (1989). A review of water re-use in flotation. *Minerals Engineering, 2*(1), 65–85.
35. Rawlings, D. E. (2005). Characteristics and adaptability of iron-and sulfur-oxidizing microorganisms used for the recovery of metals from minerals and their concentrates. *Microbial cell factories, 4*, 1–15.
36. Raza, N., Zafar, Z. I. (2013). An analytical model approach for the dissolution kinetics of magnesite ore using ascorbic acid as leaching agent. *International Journal of metals, 2013*(1), 352496.
37. Raza, N., Zafar, Z. I., Kumar, R. (2015). Leaching of natural magnesite ore in succinic acid solutions. *International Journal of Mineral Processing, 139*, 25–30.
38. Rossi, L. M., Costa, N. J., Silva, F. P., Wojcieszak, R. (2014). Magnetic nanomaterials in catalysis: advanced catalysts for magnetic separation and beyond. *Green Chemistry, 16*(6), 2906–2933.
39. Sajjad, M., Almufarij, R., Ali, Z., Sajid, M., Raza, N., Manzoor, S., ... Abdelrahman, E. A. (2024). Magnetic solid phase extraction of aminoglycosides residue in chicken egg samples using Fe_3O_4-GO-Agarose-Chitosan composite. *Food Chemistry, 430*, 137092.

40. Sharifiaghdam, M., Shaabani, E., Asghari, F., Faridi-Majidi, R. (2022). Chitosan coated metallic nanoparticles with stability, antioxidant, and antibacterial properties: Potential for wound healing application. *Journal of Applied Polymer Science, 139*(10), 51766.
41. Sherlala, A., Raman, A., Bello, M., Asghar, A. (2018). A review of the applications of organo-functionalized magnetic graphene oxide nanocomposites for heavy metal adsorption. *Chemosphere, 193*, 1004–1017.
42. Singh, V., Biswas, A. (2017). Physicochemical processing of low grade ferruginous manganese ores. *International Journal of Mineral Processing, 158*, 35–44.
43. Tong, X. C., Tong, X. C. (2011). Electronic packaging materials and their functions in thermal managements. *Advanced Materials for Thermal Management of Electronic Packaging*, 131–167.
44. Vanumamalai, S. M., Venkatachalam, S., Srinivasan, N., Dhinakar, G. (2025). Optimized hummer's method for graphene oxide: Structural properties and electrochemical applications. *Journal of Organometallic Chemistry, 1031*, 123577.
45. Wang, F., Long, G., Bai, M., Shi, Y., Zhou, J. L. (2023). Feasibility of low-carbon electrolytic manganese residue-based supplementary cementitious materials. *Science of the total environment, 883*, 163672.
46. Wang, F., Long, G., Zhou, J. L. (2023). Deep insight into green remediation and hazard-free disposal of electrolytic manganese residue-based cementitious material. *Science of the total environment, 894*, 165049.
47. Wani, A. A., Rather, R. A., Shaari, N., Khan, U., Muhammad, T., Hussain, S. M., ... Abed, A. M. (2024). Aspects of superior photocatalytic dye degradation and adsorption efficiency of reduced graphene oxide multiwalled carbon nanotubes with modified ZnO-Al_2O_3 nanocomposites. *Journal of Environmental Chemical Engineering, 12*(2), 112461.
48. Zenasni, M. A., Benfarhi, S., Merlin, A., Molina, S., George, B., Meroufel, B. (2012). Adsorption of Cu (II) on maghnite from aqueous solution: Effects of pH, initial concentration, interaction time and temperature. *Natural science, 4*(11), 856-868.
49. Zhu, S., Zhang, Y., Xin, L., Oo, K. H., Zheng, M., Ma, S., ... Chen, Y. (2024). Near-complete recycling of real mix electroplating sludge as valuable metals via Fe/Cr co-crystallization and stepwise extraction route. *Journal of Environmental Management, 358*, 120821.
50. Zou, Y., Chernyaev, A., Ossama, M., Seisko, S., Lundström, M. (2024). Leaching of NMC industrial black mass in the presence of LFP. *Scientific Reports, 14*(1), 10818.